AIP | Applied Physics Letters

High color purity ZnSe/ZnS core/shell quantum dot based blue light emitting diodes with an inverted device structure

Wenyu Ji, Pengtao Jing, Wei Xu, Xi Yuan, Yunjun Wang, Jialong Zhao, and Alex K.-Y. Jen

Citation: Applied Physics Letters **103**, 053106 (2013); doi: 10.1063/1.4817086
View online: http://dx.doi.org/10.1063/1.4817086
View Table of Contents: http://scitation.aip.org/content/aip/journal/apl/103/5?ver=pdfcov
Published by the AIP Publishing

High color purity ZnSe/ZnS core/shell quantum dot based blue light emitting diodes with an inverted device structure

Wenyu Ji,[1] Pengtao Jing,[1] Wei Xu,[1,2] Xi Yuan,[1,2] Yunjun Wang,[3] Jialong Zhao,[1,a)] and Alex K.-Y. Jen[4,b)]
[1]*State Key Laboratory of Luminescence and Applications, Changchun Institute of Optics, Fine Mechanics and Physics, Chinese Academy of Sciences, Changchun 130033, China*
[2]*University of Chinese Academy of Sciences, Beijing 100039, China*
[3]*Mesolight LLC, 4607W 61st Street, Little Rock, Arkansas 72209, USA*
[4]*Department of Materials Science & Engineering, University of Washington, Seattle, Washington 98195-2120, USA*

(Received 18 March 2013; accepted 16 July 2013; published online 30 July 2013)

Deep-blue, high color purity electroluminescence (EL) is demonstrated in an inverted light-emitting device using nontoxic ZnSe/ZnS core/shell quantum dots (QDs) as the emitter. The device exhibits moderate turn-on voltage (4.0 V) and color-saturated deep blue emission with a narrow full width at half maximum of ~15 nm and emission peak at 441 nm. Their maximum luminance and current efficiency reach 1170 cd/m^2 and 0.51 cd/A, respectively. The high performances are achieved through a ZnO nanoparticle based electron-transporting layer due to efficient electron injection into the ZnSe/ZnS QDs. Energy transfer processes between the ZnSe/ZnS QDs and hole-transporting materials are studied by time-resolved photoluminescence spectroscopy to understand the EL mechanism of the devices. These results provide a new guide for the fabrication of efficient deep-blue quantum dot light-emitting diodes and the realization of QD-based lighting sources and full-color panel displays. © *2013 AIP Publishing LLC*. [http://dx.doi.org/10.1063/1.4817086]

Colloidal quantum dot light-emitting diodes (QD-LEDs) possess superior features, such as narrow full width at half-maximum (FWHM) of ~18–30 nm and tunable emissions in the full visible spectral range, which are strongly dependent on the QD size and composition.[1–4] However, a serious drawback to the present technology is its strong dependence on the cadmium cation-based nanocrystals which bring in environmental and cost concerns. The heavy-metal nature of the cadmium composition raises concerns about carcinogenicity and other chronic health risks as well as disposal hazards.[5] A broad range of compounds and elemental semiconductors, including InP, Si, ZnSe, and ZnCuInS, have been exploited to design and synthesize colloidal QDs that are more environmental-friendly and can be used in QD-LEDs.[6–10] To date, among the three primary colors, the development of blue QD-LEDs is lagging behind their counterpart of green and red QD-LEDs in terms of device performance. Moreover, electroluminescence (EL) of blue QD-LEDs is often accompanied with trap emissions.[11–15] To make QD-LED-based displays more competitive and to further improve their quality, it is highly desirable to combine the properties of emission with higher color rendering index, greater resemblance to the sunlight spectrum, and more environmental-friendly sources. All these hinge on pure deep-blue emission. However, efficient deep-blue or even pure-blue emission with environmental-friendly material has seldom been observed from QD-LEDs.[15] When compared with CdS and CdSe QDs, ZnSe QDs have significant advantages in the UV-blue region due to the larger band gap of ZnSe (2.7 eV) than CdS (2.4 eV) and CdSe (1.74 eV). Currently, there are only a few reports on ZnSe/ZnS QD based LEDs.[8,16] However, low quantum efficiency was observed in the devices due to defect-related emissions. Therefore, the fabrication of efficient and pure ZnSe/ZnS based QD-LEDs is still a challenge.

In this study, we report the fabrication of the inverted deep-blue QD-LEDs using high quality ZnSe/ZnS core/shell QDs as the emitter. The EL emission peak of the QDs is 441 nm with a FWHM of 15.2 nm, which is significantly narrower than that of blue LEDs with Cd-based QDs. The QD-LEDs consist of glass substrates coated with ITO/ZnO (35 nm)/ZnSe/ZnS QDs (~3 monolayers (MLs))/hole transport layer (HTL) (45 nm)/MoO_3 (8 nm)/Al (200 nm). The CBP is 4,4-N,N-dicarbazole-biphenyl and TCTA is 4,4′,4″-Tris(carbazol-9-yl)-triphenylamine. The ITO glass substrates were cleaned in ultrasonic bath with isopropyl alcohol, acetone, and methanol sequentially. ZnO nanoparticles were synthesized by the previously reported method.[17] The core/shell structured ZnSe/ZnS QDs were synthesized according to previously published method.[18] Their shell thicknesses were estimated to be about 8.5 and 5.0 MLs and the photoluminescence (PL) quantum yields were determined to be about 60% and 45% for QD1 (PL peak at 439 nm) and QD2 (PL peak at 412 nm), respectively. ZnO nanoparticles dissolved in butanol with a concentration of 22 mg/ml were spin-coated at 2000 rpm and dried in glove box (MBRAUN) at 100 °C for 30 min. After that, QDs dissolved in toluene (the optical density (OD) of the QD solution was 3.2 at wavelength of 400 nm, which was estimated from the diluted solution) were deposited by spin-coating at 2000 rpm, followed by drying in glove box (MBRAUN) at 70 °C for 30 min. Then, hole transporting materials (CBP for Device A,

a)Author to whom correspondence should be addressed. Electronic mail: zhaojl@ciomp.ac.cn.
b)Electronic mail: ajen@u.washington.edu

and TCTA for Device B), MoO_3, and Al were successively deposited by thermal evaporation at pressure below 4×10^{-6} Torr. The characteristics of current-voltage-luminance and EL spectra were measured by a programmable Keithley model 2400 power supply and a Photo-research PR655 spectrometer in air at room temperature. For the time-resolved PL (TRPL) measurements, the samples were fabricated on quartz glass substrate and all the films were fabricated using the same technique described above. The TRPL measurements were carried out with the Edinburgh Instruments FL920 Spectrometer. Samples series for TRPL measurement are as follows: S-A: substrate/QD (~3 MLs), S-B: substrate/QD (~3 MLs)/CBP (7 nm), S-C: substrate/QD (~3 MLs)/TCTA (7 nm), S-D: substrate/CBP (7 nm), and S-E: substrate/TCTA (7 nm).

The absorption, PL, and EL spectra of QD1 and QD2 are shown in Figs. 1(a) and 1(b). The insets show the pictures of QD PL emission. As seen in the figures, the PL spectra with a very narrow FWHM, 11.1 nm for QD1 and 15.5 nm for QD2 are obtained and no emission from surface defect/trap states is observed, indicating high quality of the QDs. The EL spectra of the QD-LEDs are in agreement with the PL ones of the ZnSe/ZnS QDs in toluene, only showing a small increase in the FWHM from 11.1 nm to 15.2 nm and 15.5 nm to 19.1 nm for QD1 and QD2 based devices, respectively. Compared with the PL, the observed EL peaks are also slightly red-shifted from 439 nm to 441 nm and from 412 nm to 414 nm, respectively, for QD1 and QD2 based devices. It is likely that this shift originates from the Förster energy transfer from smaller dots (donor) to larger ones (acceptor) in the film or due to the electric field induced Stark effect.[19]

The detailed structure of the QD-LED and the energy level diagram of materials used in our work are shown in Figs. 2(a) and 2(b). The highest occupied molecular orbital (HOMO), lowest unoccupied molecular orbital (LUMO), conduction and valence band levels of the materials are taken from the literature.[17,20,21] The band-edge of ZnSe/ZnS QDs (with PL peak at 439 nm) determined from the optical band gap is in accordance with effective mass approximation calculations.[22] Figure 2(c) shows the EL spectra of a ZnSe/ZnS

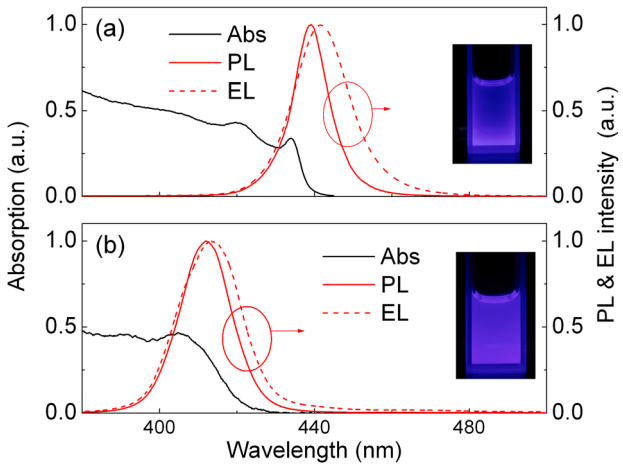

FIG. 1. The PL/absorption spectra of the two QD samples in toluene and EL spectra of QD-LEDs. Insets are the photos of QD PL.

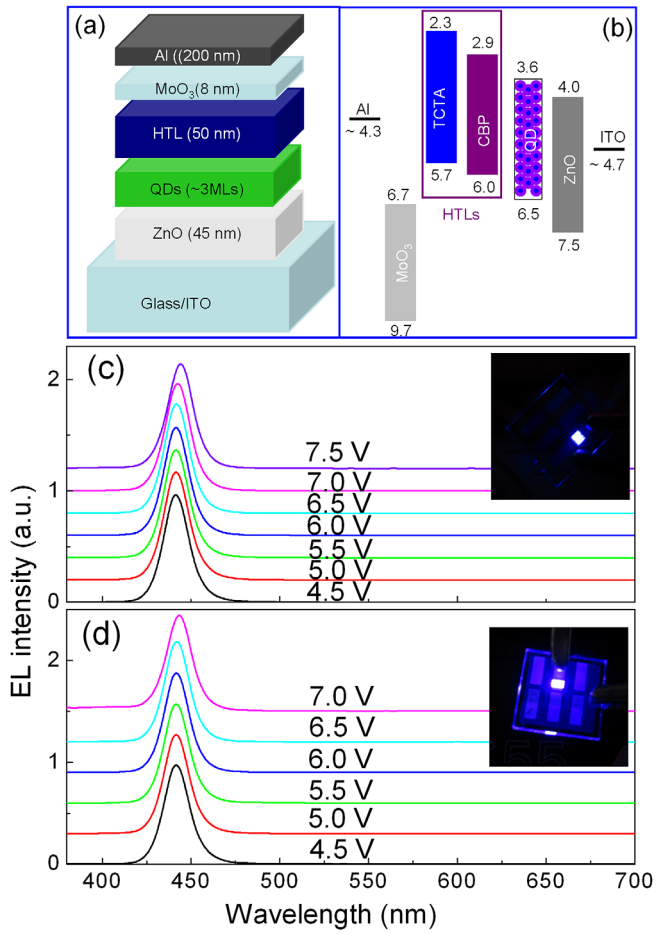

FIG. 2. (a) The structure of the QD-LED; (b) energy level diagram of the materials used in this work; (c) EL spectra of Device A under different voltages. The inset shows the photograph of Device A under operating voltage of 5.0 V; (d) the EL spectra of Device B under different voltages. The inset shows the photograph of Device B under operating voltage of 6.0 V.

QD-LED (Device A) measured at voltages from 4.5 V to 7.5 V. The EL spectral line shape of the QD-LED almost remains unchanged within the whole measured voltage range and the FWHM is as narrow as 15.2 nm. The emission bandwidth of the blue QD-LED demonstrated here is even narrower than that derived from single crystal semiconductor LEDs (such as GaN or InGaN LED at 441 nm with an emission FWHM of ~20–25 nm) and that of EL from CdS/ZnS and $Cd_{1-x}Zn_xS$@ZnS nanocrystals.[14,19] In addition, the low-energy region of the EL spectra does not exhibit any feature emission from deep-level trap states. Furthermore, there was no parasitic emission from the neighboring organic layers over the entire range of the driving voltage, which demonstrates the effective charge injection, energy transfer, and exciton recombination in the QD layer. The inset shows a photograph of the device driving at 5.0 V. The EL of our QD-LED is sufficiently bright and vivid. Figure 2(d) shows the EL spectra of Device B measured at voltages from 4.5 V to 7.0 V. As shown in this figure, pure emission from the QDs can also be observed. The spectral line shape remains almost the same as that of Device A with a narrow FWHM of 15.2 nm. The inset shows a photograph of the device driving at 5.5 V. It is valuable to note that broadening of the FWHM for the EL spectra relative to those of PL spectra is observed,

which is ascribed to the effect of electric field. The same phenomena were reported in our previous paper that the electron wave function can penetrate into the shell, causing a large spectral linewidth broadening of EL under high electric field.[23]

Figure 3(a) shows current density-voltage-luminance characteristics of devices A and B and Fig. 3(b) shows the current efficiency-current density characteristics of Devices A and B. As can be seen, the QD-LED employing CBP as HTL exhibits better performance than the device with TCTA as HTL. The device with TCTA as HTL exhibits lower luminance and efficiency at the same current density because the HOMO energy level of the TCTA is too high for hole injection into the corresponding valence band of ZnSe/ZnS QDs. Device A has a lower turn-on voltage (4.0 V, the voltage when the luminance is 1 cd/m^2) than that of Device B (4.6 V), which is attributed to better hole injection from CBP to the QD due to a lower hole injection potential energy barrier between CBP and the QD. The current density of 112 mA/cm^2 (23 mA/cm^2) and luminance of 583 cd/m^2 (76 cd/m^2) were obtained at an operation voltage of 6.0 V for Device A (B). The peak luminance of 1170 and 394 cd/m^2 was achieved for Devices A and B, respectively. The Commission Internationale de l'Enclairage (CIE) coordinates of both QD-LEDs are (0.16, 0.15) as shown in the inset in Fig. 3(b), which is the best result that has been published so far. The performance of the ZnSe/ZnS QD-LED is the best one reported to date.[8,16] The significantly improved device performance should be the result of direct exciton recombination within the QD layer due to efficient charge injection into QDs from ZnO and CBP.

Figure 4(a) shows the PL spectra of CBP and TCTA and absorption and PL spectra of ZnSe/ZnS core/shell QDs. The emission peak locates at 372 and 420 nm for CBP and TCTA in chloroform solvent at room temperature, respectively. An effective overlap between the PL spectra of HTLs and the absorption spectrum of the QDs is the prerequisite for efficient Förster resonance energy transfer.[24] In order to obtain

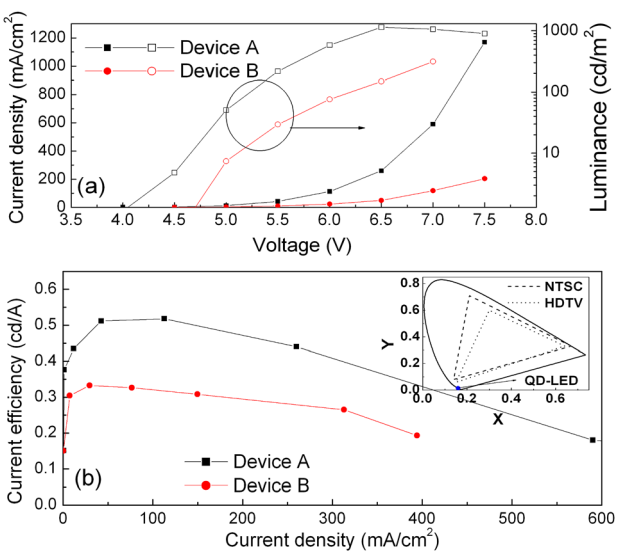

FIG. 3. (a) Current density-voltage-luminance and (b) efficiency-current density curves of devices A and B. The inset shows the CIE coordinates of the QD-LEDs with respect to the color triangle of NTSC.

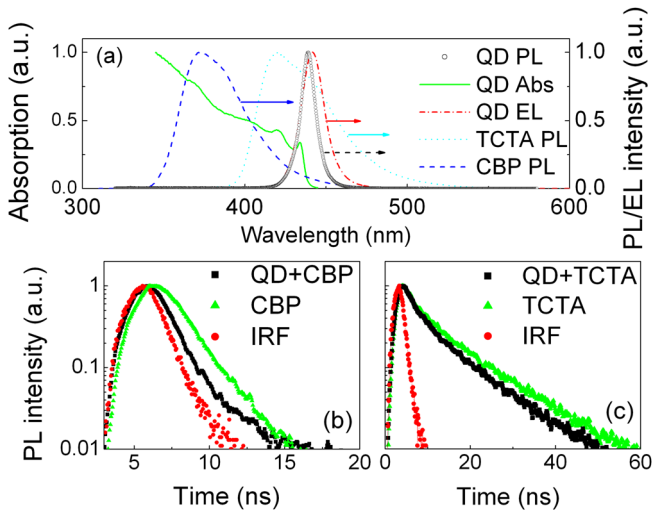

FIG. 4. (a) PL spectra of TCTA, CBP, and ZnSe/ZnS QDs and absorption spectrum of the QDs in toluene; (b) and (c) represent the TRPL of CBP in QD/CBP and TCTA in QD/TCTA films, respectively.

quantitative energy transfer efficiency from HTLs to QDs, we have measured the PL lifetimes of HTLs, CBP, and TCTA, in samples S-B, S-C, S-D, and S-E through TRPL as shown in Figs. 4(b) and 4(c).

The PL dynamic signal was collected at 372 and 410 nm under an excitation wavelength of 300 nm for CBP and TCTA, respectively. Here, we selected PL dynamic signal at 410 nm for TCTA to eliminate the effect of the QD emission on the TCTA lifetime measurement. Fitting the TRPL spectra by convoluting the instrument response function (IRF) with a bi-exponential equation, the average PL lifetime of neat TCTA (τ_{TCTA}) and CBP (τ_{CBP}) was estimated to be 12.13 and 1.25 ns, respectively. The average PL lifetime of TCTA in Sample S-C ($\tau_{TCTA+QD}$) and CBP in Sample S-B (τ_{CBP+QD}) was estimated to be 10.68 and 0.72 ns, respectively. We calculated the energy transfer efficiency from the two HTLs to QD layer by measuring the PL lifetime of HTLs in Samples S-B, S-C, S-D, and S-E. The energy transfer efficiency ($\eta_{ET} = 1 - \tau_{HTL+QD}/\tau_{HTL}$, τ_{HTL} and τ_{HTL+QD} is the PL lifetime of HTLs in S-B/S-C and S-D/S-E, respectively) was calculated to be 12% and 42% from TCTA and CBP to the QDs, respectively.[24] It is worthy to note that although the energy transfer efficiency from TCTA to QD is only 12%, the EL emission in Device B is from QDs but is not from TCTA under the operating voltage from 4.5 V to 7.0 V. In other words, the EL emission for Device B entirely originates from the QDs from the luminance of ~1 cd/m^2 to the maximum luminance, ~400 cd/m^2. This means that the dominant EL emission in Device B comes from charge injection rather than energy transfer from TCTA to the QD layer. Otherwise, if the energy transfer is the primary mechanism in the QD-LED, the emission from TCTA will be clearly observed due to the low energy transfer efficiency. In addition, the barrier height for hole injection from TCTA to QD is ~0.8 eV, which is smaller than that for electron injection from QDs into HTLs (~1.3 eV), the majority of excitons are formed in the QDs. The similar result is also obtained for CBP based device. Here, all the results suggest that the operating mechanism of the devices is mainly attributed to the direct charge injection. The excellent performance of the

CBP based device is also ascribed to the more efficient hole injection from CBP to QD layer compared to that from TCTA to QDs due to the lower HOMO energy level of CBP as shown in Fig. 2(b).

Furthermore, the charge balance of devices should be an important factor to influence the performance of our QD-LEDs. In our devices, the electron transport and injection into QDs are favored due to low conduction band and good electron mobility of ZnO film ($\mu_e \sim 1.3 \times 10^{-3}$ $cm^2V^{-1}s^{-1}$).[17] For hole injection and transport into QDs, CBP is superior to TCTA owing to its higher HOMO energy level and hole mobility (1×10^{-3} cm^2 $V^{-1}s^{-1}$ and 4×10^{-4} $cm^2V^{-1}s^{-1}$ for CBP and TCTA, respectively).[25,26] Such a difference in carrier injection and transport should cause charge imbalance in TCTA based device, resulting in low electron-hole radiative recombination efficiency. An imbalanced charge transport also leads to the charging of QDs and strong non-radiative Auger recombination in the QD layer where an exciton recombines nonradiatively by transferring its energy to an unpaired carrier that then relaxes to the ground state via interactions with phonons. In the TCTA-based device, generated excitons are likely to be quenched by excess electrons due to few holes injected into the QD layer. In addition, the excellent performance of ZnSe/ZnS QD-LEDs is related to high quality core/shell QDs with a small number of surface defect/trap states due to overcoating of a thick ZnS shell ($\sim$ 8.5 MLs). As reported by *Galland*, the QDs with a thick shell have higher quantum yields during OFF periods than those of standard nanocrystals.[27] Furthermore, it has been recently reported that the thick CdS shell coated CdSe QDs with significantly suppressed blinking and high PL quantum efficiency exhibit high external quantum efficiency and luminance in QD-LEDs.[28–30]

In summary, we have fabricated deep-blue QD-LEDs with an inverted structure using colloidal ZnSe/ZnS core/shell QDs as the emitter. These inverted devices represent the state-of-the-art blue-emitting QD-LEDs with heavy-metal-free and nontoxic QDs, deep-blue (EL peak at 441 nm), and extremely narrow (FWHM $\sim$ 15.2 nm) EL emission with ultrahigh color purity [CIE coordinates are (0.16, 0.015)], maximum luminance of 1170 cd/m^2, and peak current efficiency of 0.51 cd/A. This work demonstrates the potential for colloidal ZnSe/ZnS nanocrystals as blue emitters for LEDs and the pure QD band gap emission. No EL emission from organic materials or surface defect/trap states of the QDs is observed. More efficient devices await additional and further studies, but the present findings demonstrate some of the benefits of using an inverted structure for QD-LEDs.

This work was supported by the Hundred Talent Program of the Chinese Academy of Sciences and the National Natural Science Foundation of China (Nos. 61205025, 11274304, and 11204298).

[1]S. Coe, W.-K. Woo, M. G. Bawendi, and V. Bulović, Nature **420**, 800 (2002).
[2]J. S. Steckel, J. P. Zimmer, S. Coe-Sullivan, N. E. Stott, V. Bulović, and M. G. Bawendi, Angew. Chem., Int. Ed. **43**, 2154 (2004).
[3]V. Wood and V. Bulović, Nano Rev. **1**, 5202 (2010).
[4]Y. Shirasaki, G. J. Supran, M. G. Bawendi, and V. Bulović, Nat. Photonics **7**, 13 (2013).
[5]B. Sarkar, *Heavy Metals in the Environment* (CRC Press, Boca Raton, FL, 2002).
[6]X. Yang, D. Zhao, K. S. Leck, S. T. Tan, Y. X. Tang, J. Zhao, H. V. Demir, and X. W. Sun, Adv. Mater. **24**, 4180 (2012).
[7]D. P. Puzzo, E. J. Henderson, M. G. Helander, Z. Wang, G. A. Ozin, and Z. H. Lu, Nano Lett. **11**, 1585 (2011).
[8]S. C. De and S. S. Nath, J. Lumin. **131**, 2707 (2011).
[9]Z. Tan, Y. Zhang, C. Xie, H. Su, J. Liu, C. Zhang, N. Dellas, S. E. Mohney, Y. Wang, J. Wang, and J. Xu, Adv. Mater. **23**, 3553 (2011).
[10]B. K. Chen, H. Z. Zhong, W. Q. Zhang, Z. A. Tan, Y. F. Li, C. R. Yu, T. Y. Zhai, Y. Bando, S. Y. Yang, and B. S. Zou, Adv. Funct. Mater. **22**, 2081 (2012).
[11]P. O. Anikeeva, J. E. Halpert, M. G. Bawendi, and V. Bulović, Nano Lett. **9**, 2532 (2009).
[12]T. H. Kim, K. S. Cho, E. K. Lee, S. J. Lee, J. Chae, J. W. Kim, D. H. Kim, J. Y. Kwon, G. Amaratunga, S. Y. Lee, B. L. Choi, Y. Kuk, J. M. Kim, and K. Kim, Nat. Photonics **5**, 176 (2011).
[13]L. Kim, P. O. Anikeeva, S. Coe-Sullivan, J. S. Steckel, M. G. Bawendi, and V. Bulovic, Nano Lett. **8**, 4513 (2008).
[14]Z. Tan, F. Zhang, T. Zhu, J. Xu, A. Y. Wang, J. D. Dixon, L. Li, Q. Zhang, and S. E. Mohney, Nano Lett. **7**, 3803 (2007).
[15]H. B. Shen, H. Z. Wang, X. M. Li, J. Z. Niu, H. Wang, X. Chen, and L. S. Li, Dalton Trans. **47**, 10534 (2009).
[16]C. Xiang, W. Koo, S. Chen, F. So, X. Liu, X. Kong, and Y. Wang, Appl. Phys. Lett. **101**, 053303 (2012).
[17]J. H. Kwak, W. K. Bae, D. G. Lee, I. Park, J. H. Lim, M. J. Park, H. D. Cho, H. J. Woo, D. Y. Yoon, K. H. Char, S. H. Lee, and C. H. Lee, Nano Lett. **12**, 2362 (2012).
[18]Y. Wang, X. Liu, X. Kong, J. Wang, and A. Barton, USPTO Provisional patent application 61,606,700.
[19]J. L. Zhao, J. Y. Zhang, C. Y. Jiang, J. Bohnenberger, T. Basche, and A. Mews, J. Appl. Phys. **96**, 3206 (2004).
[20]T. Y. Zhang, M. Liu, T. Li, J. Ma, D. L. Liu, W. F. Xie, C. L. Wu, S. W. Liu, S. C. Yeh, and C. T. Chen, J. Phys. Chem. C **115**, 2428 (2011).
[21]J. Meyer, S. Hamwi, M. Kröger, W. Kowalsky, T. Riedl, and A. Kahn, Adv. Mater. **24**, 5408 (2012).
[22]J. Xia, Phys. Rev. B **40**, 8500 (1989).
[23]P. Jing, J. Zheng, Q. Zeng, Y. Zhang, X. Liu, X. Liu, X. Kong, and J. Zhao, J. Appl. Phys. **105**, 044313 (2009).
[24]J. R. Lakowicz, *Principles of Fluorescence Spectroscopy*, 3rd ed. (Springer, Berlin, Heidelberg, 2006), pp. 443–527.
[25]H. I. Baek and C. Lee, J. Appl. Phys. **103**, 054510 (2008).
[26]S. Noh, C. K. Suman, Y. Hong, and C. Lee, J. Appl. Phys. **105**, 033709 (2009).
[27]C. Galland, Y. Ghosh, A. Steinbrück, M. Sykora, J. A. Hollingsworth, V. I. Klimov, and H. Htoon, Nature **479**, 203 (2011).
[28]P. Spinicelli, S. Buil, X. Quelin, B. Mahler, B. Dubertret, and J. P. Hermier, Phys. Rev. Lett. **102**, 136801 (2009).
[29]B. Mahler, P. Spinicelli, S. Buil, X. Quelin, J.-P. Hermier, and B. Dubertret, Nature Mater. **7**, 659 (2008).
[30]B. N. Pal, Y. Ghosh, S. Brovelli, R. Laocharoensuk, V. I. Klimov, J. A. Hollingsworth, and H. Htoon, Nano Lett. **12**, 331 (2012).